In-process ink rheology monitoring for inkjet printing using piezo self-sensing

Filliger Sebastian, Brügger Luca, Piller Julian, Perritaz Gaël, Bullot Loïc, Chabert Ull Carlos

iPrint, Route de l'Ancienne Papeterie 180, 1723 Marly Switzerland
HEIA-FR, HES-SO University of Applied Sciences and Arts Western Switzerland

Abstract

Inkjet is gaining popularity in digital production for its high flexibility, productivity and compatibility with many substrates. The core of the inkjet system is the printhead, a sophisticated device depositing ink accurately and on demand through thousands of independent nozzles. However, the complexity of the printhead presents challenges for maintenance and stable operation. Therefore, maintaining precise control over all process parameters is essential to ensure consistent quality and optimal performance.

Ink rheology is an important process parameter to control. Changes in rheology caused by solvent evaporation, ink aging, sedimentation or simply a slightly different formulation of the manufacturer can lead to major quality flaws in the printing process. Commercial solutions for rheology measurements can typically only measure viscosities at frequencies of up to 10 kHz and the measurement takes place outside of the printing process.

Here, a measurement system has been developed, which can monitor the rheology in the process at internal resonance frequencies of 100-200 kHz using only the printhead as the measurement device together with printing electronics which has piezo self-sensing capabilities. This system is an upgrade to a previously developed and industry tested nozzle status monitoring system that uses the piezoelectric effect to map printhead internal acoustics for nozzle failure detection.

Introduction

Issues with ink and ink delivery systems are common in demanding printing processes. Solvent evaporation, aging of ink, sedimentation, changes in particle loading, chemical incompatibility and ink formulation deviations between batches can lead to major flaws in the the printing process. In the present work, a system to monitor changes in ink rheology during the printing process has been developed. This rheology measurement is done at frequencies specifically relevant for the printing process which lay beyond $100\,kHz$.

Materials and Methods

The capability of a piezoelectric crystal to convert electrical energy into mechanical energy is the underlying principle of piezo based inkjet technology. The piezo actuator acts onto the ink and presses ink out of the nozzle to form a drop flying towards a substrate. This energy conversion is reversible, enabling the measurement of pressure from acoustic waves within the inkjet nozzle as they act on the piezo. These pressure waves not only respond to the actuation process but also reflect the condition of the fluidic system. Consequently, they offer a valuable means to detect various issues and assess the properties of the fluidic system.

The piezoelectric effect couples the electrical and mechanical part of the printhead due to its reversibility. The electrical side involves notably the output impedance of the printing waveform amplifier, cable and ASIC parasitics, and the capacitance of the piezo actuator. The mechanical part encompasses the properties of the actuator, the vibrating diaphragm, and the response of the fluidic system.

Creating a detailed model for the fluidic part can be quite complex, especially when a precise match with a real printhead is required [1]. However, to grasp the measurement approach, we don't need to delve into this complexity. In this study, we simplified the mechanical part of the printhead as a basic damped resonator as a good enough approximation.

The damped resonator, a mechanical part, can be modeled as an electrical circuit. This resonator is coupled with the piezo actuator over a coupling constant as shown in figure 1.
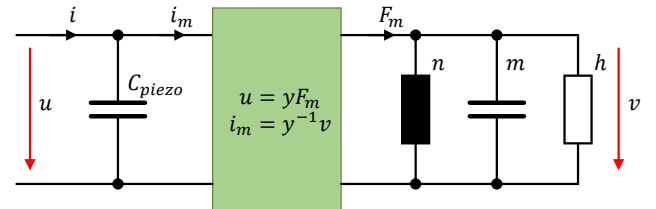

Figure 1. *Electrical model of coupled system consisting of fluidic resonator and piezo actuator [2]*

Where:

C_{piezo} : Electrical capacitance of the piezo

n : Mechanical compliance of the system

m : Effective mass of the system

h : Intrinsic loss of the system

i, u : Electrical current and voltage

F_m, v : Mechanical force and velocity

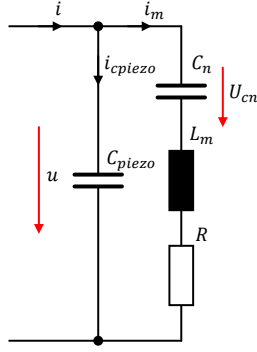The coupled system in figure 1 can be simplified to the equivalent electric circuit shown in figure 2.

Figure 2. *Equivalent electrical scheme of the piezo actuator with coupled mechanical damped resonator*

The viscosity and other mechanical losses are responsible for the loss of energy in the resonator. The viscosity appears in part as the resistive element of a resonant circuit when characterising the piezo actuator and coupled mechanical parts. By measurement of the electric impedance it is therefore possible to determine the viscosity. In a next step the measurement approach is discussed.

Applying a changing voltage to the piezo will result in a current i_{cpiezo} flowing through the plate capacitor formed by the physical structure of the actuator. The mechanically coupled part of the actuator will introduce an additional current i_m. Considering the two port model of an electro-acoustic system [3] (equation 1), isolating (equation 2) and deriving the equation for the piezo charge shows that the current into the piezo can be interpreted as consisting of above mentioned two components i_{cpiezo} and i_m (equation 3).

$$\begin{pmatrix} \Delta Vol \\ q \end{pmatrix} = \begin{bmatrix} C_{AS} & d_A \\ d_A & C_{EF} \end{bmatrix} \begin{pmatrix} P \\ V \end{pmatrix} \qquad (1)$$

Where:

ΔVol : Volume displacement

q : Electric charge of piezo

C_{AS} : Short-circuit acoustic compliance

d_A : Effective acoustic piezoelectric coefficient

C_{EF} : Electrical free capacitance of the piezoelectric material

P : Pressure on piezo surface

V : Voltage over piezo

$$q = d_A P + C_{EF} V \qquad (2)$$

$$i = \frac{dq}{dt} = d_A \frac{dP}{dt} + C_{EF} \frac{dV}{dt} = i_m + i_{cpiezo} \qquad (3)$$

Experiments conducted at iPrint by the authors and other researchers [4] show that i_{cpiezo} can be 100 to 1000 times larger than i_m during a changing waveform. Therefore, i_{cpiezo} must be suppressed to allow a measurement of pressure. In piezo self sensing a common workaround is to do the measurement only during a phase of constant voltage of the driving waveform,

mostly some µs after the driving pulse has ended [5]. In this case $\frac{dV}{dt}$ is zero and therefore i_{cpiezo} as well.

This method was not applicable in this study because the excitation of the piezo actuator was sinusoidal and stationary. The current i_{cpiezo} was removed by generating an identical current and subtracting it analogically from the current through the piezo capacitance (figure 3). This approach has been proposed before [6]. A capacitor was tuned to the exact same capacitance of the actuator. In addition, cabling, layout, connectors and input impedance of the printhead ASIC need to be matched as well.
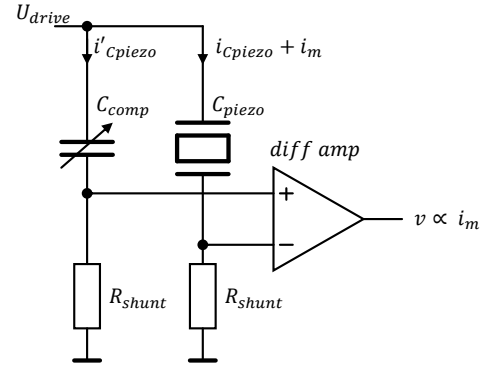

Figure 3. *Electrical circuit for pressure change measurement with compensation*

All discussed above lead to the measurement circuit shown in figure 4. By direct digital synthesis a sinus was generated to excite the actuator and a tuneable reference capacitor simulating the actuator capacitance and other parasitics. The currents were compared first passing through an isolated shunt amplifier to achieve excellent common mode rejection at high frequencies followed by a difference amplifier and a logarithmic amplifier to compress the dynamic range to reduce requirements of the data conversion.
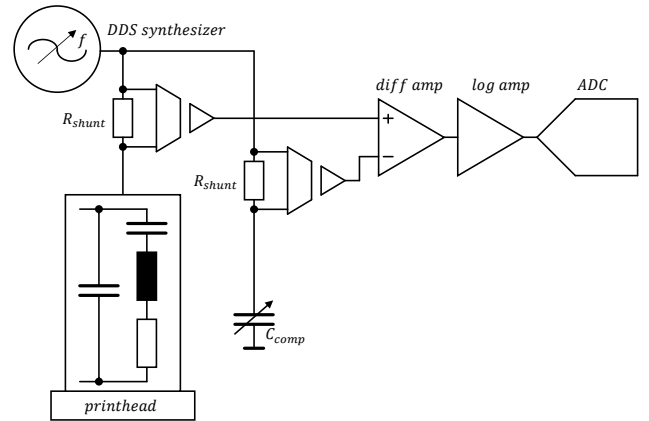

Figure 4. *Complete measurement system*

The circuit in figure 5 shows the major resonating elements. Parallel and serial resonance circuits are present indicating that we will obtain peaks of maximum measured current and anti peaks with minimal measured current. It is very important to note that the elements forming the mechanically coupled part of the circuit will change depending on the state of the fluidic system. It was impossible during this study to properly measure the electric equivalents of said elements.
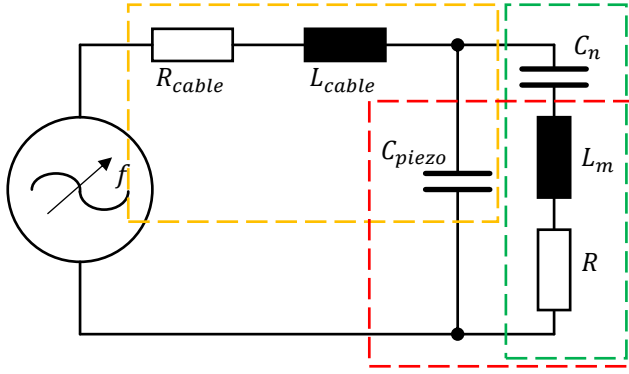
Figure 5. *Series resonances marked in yellow and green and parallel resonances marked in red*

The laboratory tests required carefully selected test fluids. The selection of fluids is based on the following considerations:

- Only few rheological measurement devices can measure viscosity at elevated frequencies. The highest ranging device available to the authors was the TriPAV, measuring up to $10\,kHz$. Newtonian fluids are chosen so that the viscosity outside of the measurement range of the used device can be assumed to remain the same.
- In this study only the viscosity of the ink is of interest. Other parameters of the ink that change the resonance behaviour must remain identical.

To understand how to select inks, the governing equations of fluidic motion inside the printhead must be understood. The simplified model of an ejection unit in figure 6 [1] shows the principal elements. The nozzle, a tube with an interface between ink and air called the meniscus. The nozzle chamber with an attached actuator that can change the volume of the chamber. A restrictor, which is a simple tube separating the nozzle chamber and the ink manifold. Below the most important physical laws in play are discussed.
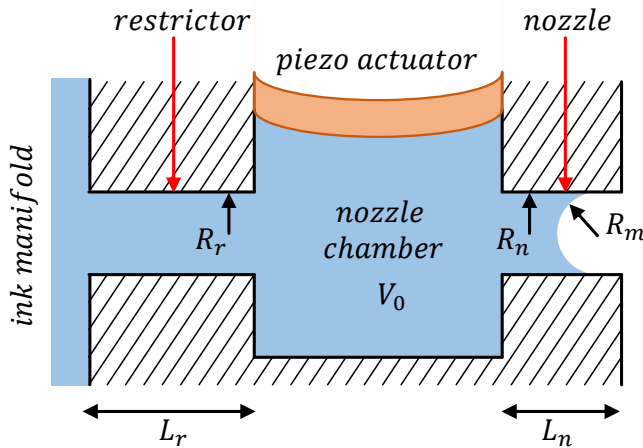

Figure 6. *Schematic view of an inkjet ejection unit called "the nozzle"*

The meniscus forms an elastic element due to its surface tension. If the meniscus is pushed out, then the positive curvature will exert a positive pressure back onto the ink and vice versa when bent inwards. According to Young's law the pressure created by a curved surface of liquid in contact with air is:

$$\Delta p_m = \frac{2\gamma}{R_m} \tag{4}$$

Where:

Δp_m : Pressure created by meniscus surface tension

γ : Surface tension

R_m : Radius of meniscus curvature

Movement of a fluid through a channel creates friction. The Hagen-Poiseuille law describes the relation between pressure and flow through a cylindrical tube, in this case the nozzle and the restrictor. This pressure will oppose movement of ink.

$$\Delta p = \frac{8\mu L_n}{\pi R_n^4}Q \tag{5}$$

Where:

Δp : Pressure difference through tube

μ : Dynamic viscosity

L_n : Length of tube, in this case nozzle

R_c : Radius of channel

Q : Volume flow of fluid

The nozzle chamber contains liquid with finite compressibility. A change of volume will result in a pressure change for instance when the actuator is moving. The Newton-Laplace Equation links pressure, density and speed of sound and can be developed to expression 6.

$$\Delta p = \frac{\rho_0 c^2}{V_0}\Delta V \tag{6}$$

Where:

Δp : Pressure difference in nozzle chamber

ρ_0 : Density of fluid under ambient conditions

c : Speed of sound in fluid in nozzle chamber

V_0 : Initial volume of nozzle chamber

ΔV : Volume change of nozzle chamber

The last element is the inertia of the ink in the restrictor and nozzle (inertia of ink in the nozzle chamber can be neglected due to slow movement due to large surface of conduit).

$$F = ma \Rightarrow P = L_{n,r}\rho a \tag{7}$$

with: $\quad m = A_{n,r}L_{n,r}\rho \quad$ and $\quad F = A_{n,r}P \tag{8}$

Where:

P : Pressure in nozzle or restrictor

$L_{n,r}$: Length of nozzle or restrictor

ρ : Density of fluid

a : Acceleration of ink in nozzle or restrictor

Using the expressions 4, 5, 6 and 7 and using the nozzle model in figure 6 the oscillator model in figure 7 can be developed. Solving the underlying equations and finding solutions is not necessary to understand which fluid properties influence the oscillatory behaviour of the nozzle. The following fluidic parameters occur in the equations:

γ : Surface tension

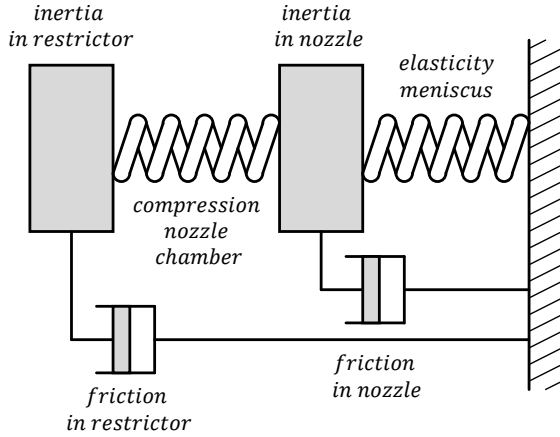μ : Dynamic viscosity

ρ : Density of fluid

Figure 7. Mechanical representation of coupled oscillator model

For this reason, test fluids of different viscosities, but as close as possible in terms of surface tension and density, were selected. Ideally, the resonance frequency should remain equal because sensitivity of the measurement circuit can be different at different frequencies.

To be able to adapt the viscosity easily a mixture of DPM (di(propylene glycol) methyl ether), TPM (tri(propylene glycol) methyl ether) and Glycerine was used to formulate all model fluids.

Figure 8 shows the complex viscosity measurements of the test fluids form $100\,Hz$ to $1\,kHz$. The response was considered flat enough to be Newtonian. Unfortunately, there exists no means of measurement available to the authors to test the viscosity at the internal resonance frequency of the nozzle.

The dynamic surface tension for surfaces ages between $5\,ms$ and $10\,s$ has been measured and revealed the same behaviour over surface age for all model fluids. The maximum deviation is $\pm 2\,mN/m$ for a surface tension of $44\,mN/m$ at an age of $5\,ms$. The relevant surface tension for the rheology measurement is in the range of microseconds. The authors did not have access to a measurement device able to measure surface tension at such small time scales. But the similar behaviour over a wide range of surface ages suggests that the model fluids will behave in a similar way also for shorter times.

Fluid	Formulation in % DPM/TPM/Glycerin	Viscosity at $1\,kHz$	Density in g/cm^3
MF1	57/38/5	6 mPas	0.98
MF2	54/36/10	8 mPas	0.982
MF3	51/34/15	9 mPas	0.983
MF4	48/32/20	15 mPas	1.008
MF5	45/30/25	21 mPas	1.022

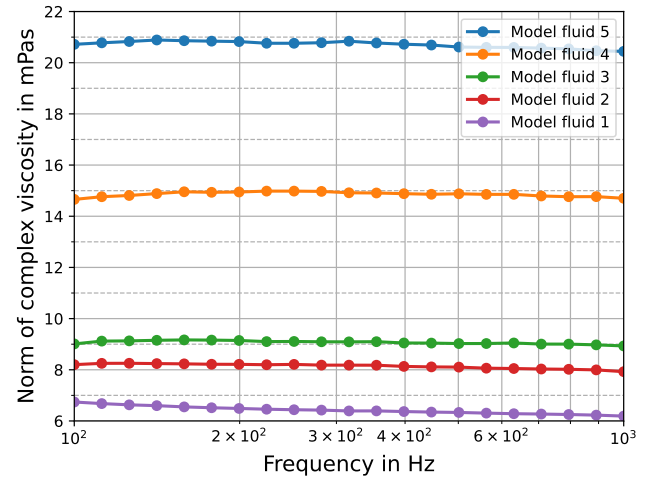**Formulation of model fluids and measured viscosity and density**

Figure 8. TriPAV measurement of the model fluids from $100\,Hz$ to $1\,kHz$

The complete measurement setup in figure 9 comprises a printhead with three connected systems:

- Fluid supply system : Ink supply with pressure and temperature regulation of ink
- Nozzle selection unit : Digital interface to select one or multiple nozzles of the printhead that are used for the rheology measurement
- Measurement unit : Electronic circuit to activate the actuator of the selected nozzles and measure the amplitude of the excited acoustic pressure wave
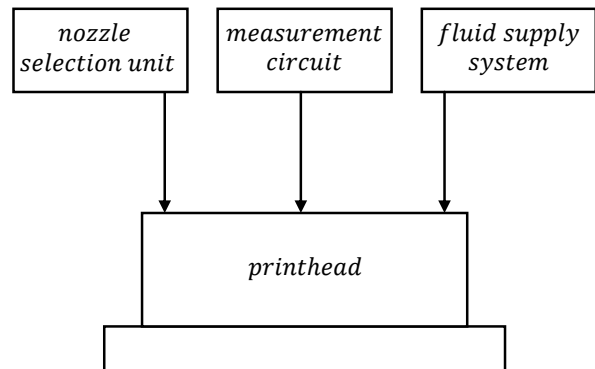

Figure 9. Block diagram of measurement setup

The fluid supply system provides stable pressures, ink flow rates and ink temperatures. Temperature control is very critical due to high temperature dependency of viscosity and actuator capacitance. Change of actuator capacitance will imbalance the electronic compensation circuit discussed above and lead to bad suppression of visible non-fluidic contributions in the measurement. Stable pressures are required to stabilise the shape of the meniscus. Changes of meniscus position will change resonance behaviour. Strong deviations from pressure target value can lead to ink dripping out of the printhead or air being aspirated in.

Figure 10 shows the fluid supply system consisting of two air pressure regulators providing stable pressures at the inlet and outlet of the printhead (P_1 and P_2). Together with a regulation of the ink level, constant hydraulic pressure at the inlet and outlet of the printhead are achieved. A difference of both pressure will result in flow through the printhead. Ink coming out of the

printhead is pumped to the inlet to allow continuous flow. Two reservoirs at the inlet and outlet allow for damping of pressure oscillations of the pump. These reservoirs are temperature controlled. The circulation of the ink together with insulated tubing and reservoirs result in constant temperature throughout the system.
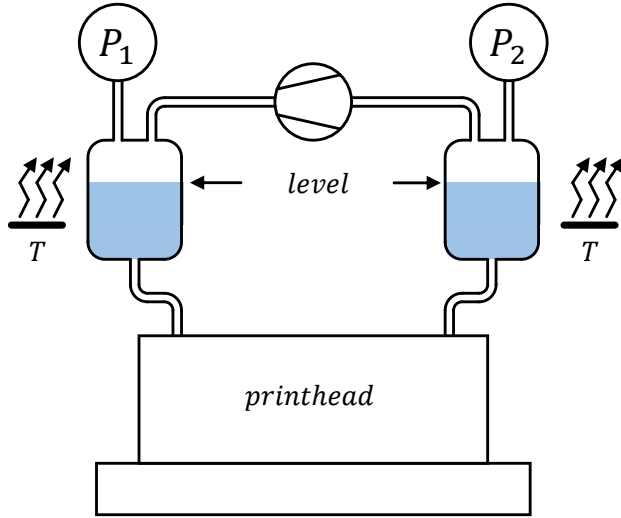

Figure 10. *Ink supply system for the printhead*

The nozzle selection unit is a custom built electronics that can interface a number of different printheads due to a modular approach. The measurement unit is custom built as well.

The final element is the printhead. In this study the Ricoh MH5420 printhead was used. The main limitation in terms of printhead selection is the access to the analogue driving waveforms of the actuators. Basically, a direct electrical connection to the actuator is required for the measurement. If this is the case, then other printheads can be used for the measurement. Preliminary tests have also been done for Dimatix Polaris and Dimatix Sapphire printheads as well as Epson S800. From a technical point of view other printheads should work as well. At this point it is important to stress that no printhead has been modified. If modifications of the printhead are possible, then even printheads with purely digital interface can be used for rheology sensing as observed in a proof of concept study at iPrint.

The test starts by cleaning the printhead. It is of utmost importance to remove the previous fluid completely which is difficult due to the microscopic size of the channels. The printhead is purged with air to remove previous fluid. Then IPA is circulated through the printhead for $5\,min$ to dissolve ink remainders. The IPA is purged with air and the printhead then dried.

At this stage a measurement is done without ink to get the behaviour of the electric and mechanical part without fluidic contributions. After this the printhead is primed with the test fluid and the actual measurement is done. These steps are repeated for all test fluids.

The actual impedance measurements starts at one frequency. A sinusoidal wave with very low amplitude is applied to one piezo actuator. The low amplitude is required to prevent self heating of the actuator and subsequently the ink. This excitation is held for $10\,ms$ and after this period the output voltage of the logarithmic amplifier is digitised. The process is repeated for the next frequency point up until the maximum frequency. Test frequencies are spaced logarithmically with 200 points per decade.

To determine the frequency range of the analysis, a first test over the entire range of the measurement circuit ($50\,kHz$ to $1.563\,MHz$) was done with and without ink (see figure 11). Without ink there are two phenomena visible. For low frequencies the measured amplitude rises with frequency. This is due to decreasing common mode rejection of the measurement circuit at higher frequencies. At about $1\,MHz$ a pronounced resonance is visible. It was not possible to determine what causes this resonance but its existence in an empty printhead suggests an electric or mechanical origin. The same measurement is repeated with ink. A pronounced resonance appears at about $120\,kHz$ which is the expected natural resonance frequency of the nozzle chamber. Harmonics of this resonance appear as well. The frequency range for subsequent measurements was arbitrarily chosen between $50\,kHz$ and $500\,kHz$ to cover the main fluidic resonance and the first harmonic.
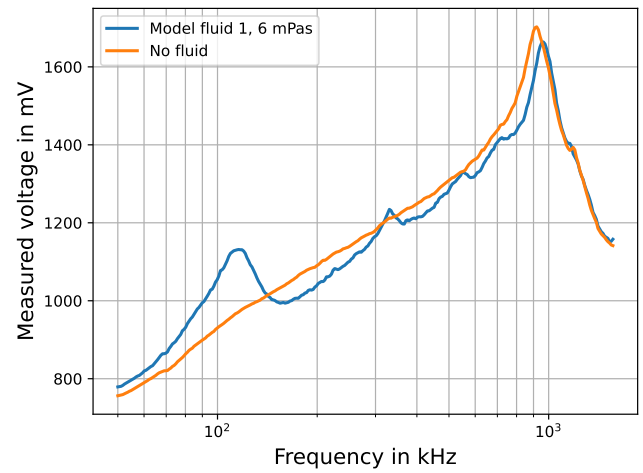

Figure 11. *Comparing the measurement without a fluid and with model fluid MF1 over the full frequency range of the measurement, with a total of 300 measurement points from $50\,kHz$ to $1.563\,MHz$*

The approach adopted in this study to extract rheology data involves fitting a function to the measurement data. The coefficients of this fitting function can subsequently be analyzed and correlated to fluidic properties. The Lorentzian function, a commonly used mathematical description for physical resonances [7], is employed.

The shape of the measured curve (see figure 11), displaying a combination of a resonance and a counter-resonance led to the choice of utilizing two Lorentzian functions in combination with an offset [8]. The formula used for this fitting process is as follows:

$$y(f) = a_1 \cdot \frac{q_1}{(f-f_0)^2 + q_1^2} + a_2 \cdot \frac{q_2}{(f-f_0)^2 + q_2^2} + m \quad (9)$$

Ultimately, the parameters for the fitting function were computed for the Newtonian model fluids.

Results

In figure 12, the frequency response of the magnitude of the pressure while excited with a stationary sinusoidal wave is shown for all model fluids. The magnitude unit is mV which is the reading of the logarithmic amplifier. It is not possible to link this value to the actual pressure inside the printhead because the electro-mechanical coupling is not known. The figure shows a

pronounced resonance peak at about $115\,kHz$. As expected, for lower viscosities the height of the peak and generally the quality factor of the resonance is higher.
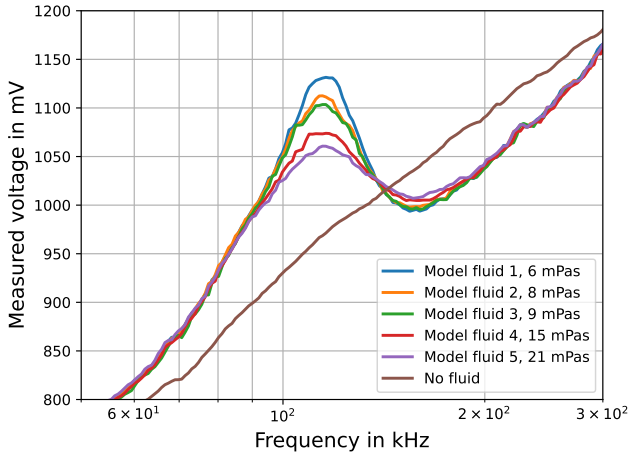

Figure 12. *Measurement results for the different model fluids using the developed setup with a total of 156 measurement points shown on the graph, reaching from $50\,kHz$ to $300\,kHz$*

The measured curves were fitted with the function shown in equation 9 and the values in table below were obtained.

Coefficient	MF1	MF2	MF3	MF4	MF5
a_1	41482	36054	32550	23943	21182
a_2	-36443	-31138	-27958	-20033	-18166
f_{o1}	124	123	121	117	114
f_{o2}	131	130	130	129	128
q_1	41	44	44	51	54
q_2	42	46	47	57	64
m	-45	-44	-45	-40	-33

Fitting coefficients obtained from fitting graphs in figure 12 with function in equation 9.

As mentioned before, the current i_{piezo} (see figure 3) is subtracted from the measurement to remove contributions due to the capacitive behaviour of the piezo from the measurement. An accurate matching of the capacitance value is indispensable. Tuning of the compensation can be done in discrete steps by adding capacitors with binary spacing. In figure 13, the result of good and bad compensation can be seen. In the case of bad compensation, more signal amplitude is measured due to non ideal common mode rejection. The non rejected common mode signal can be so high that the resonance peak is invisible. Better compensation will lower the unwanted amplitude contribution until the fluidic contribution becomes dominant and measurements are possible.
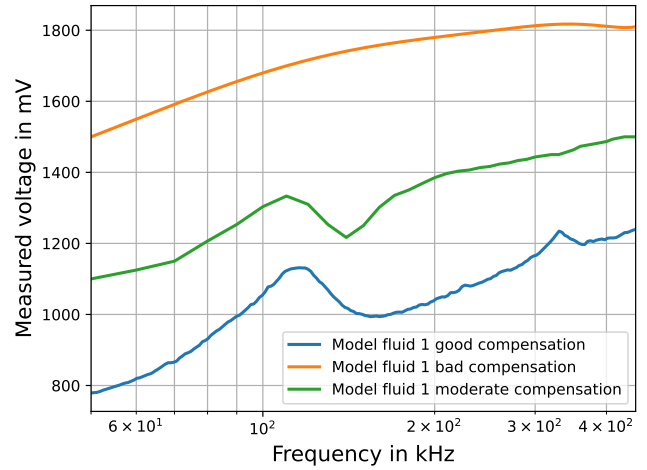

Figure 13. *Example of good, moderate and bad piezo capacitance compensation and its influence on the visibility of the resonance peak, with a total of 190 measurement points from $50\,kHz$ to $450\,kHz$*

The analysis of fitting functions to fit the amplitude of the resonance revealed an exponential decrease in the amplitude coefficient a_1 of the first Lorentzian function (resonance peak) with rising viscosity.

Consequently, another fitting function was applied to establish the relationship between viscosity and this particular amplitude coefficient. This leads to the following equation:

$$a_1(\eta) = a \cdot e^{\frac{-(\eta-b)}{c}} + d \tag{10}$$

The fitting function for the correlation between the resonance measurement fitting parameter a_1 and the viscosity looks as follows:
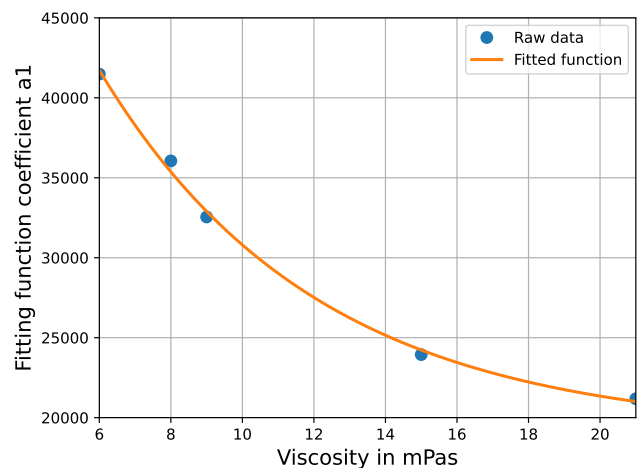

Figure 14. *Representation of the coefficient a_1 from the fitting function, as a function of the viscosity, compared to the actual measurements, the coefficient of determination is 0.9973*

The parameters that provide the best fitting are:

$$a = 40018$$
$$b = 2.54$$
$$c = 6.07$$
$$d = 19094$$

The inverse function can be used to calculate the viscosity of an unknown fluid's resonance measurement, provided that the fluids have the same density and surface tension:

$$\eta(a_1) = \ln\left(\frac{a}{a_1 - d}\right) \cdot c + b \qquad (11)$$

In addition to exploring the Lorentzian function, attempts were made to fit the data using both Gaussian and Voigt functions. The Gaussian function yielded inaccurate results, while the Voigt function provided a fitting with superior accuracy compared to the Lorentzian function. However, it is worth noting that the Voigt function demands careful consideration due to its requirement for two parameters to calculate the resonance peak, making the fitting process more intricate.

Testing to fit different coefficients versus viscosity revealed that the coefficient a_1 did result in the most accurate fitting. Which coefficient is best suited will depend on the underlying model fitted onto the measured data and in a second step the function used to fit the coefficient. Only the Lorentzian function has been investigated. The fitting of a_1 is shown in figure 14. The resulting parameters are listed in table .

In a further step, a Newtonian fluid with an unknown viscosity was calculated using the above model. The resonance curve of the unknown fluid was fitted and a coefficient $a_1 = 25328$ was obtained. Using equation 11 and coefficients from table gave a viscosity of $13.8\,mPas$. The same ink was measured to have a viscosity of $13\,mPas$ to $13.5\,mPas$ between $100\,Hz$ and $1\,kHz$ using the TriPAV high frequency rheometer.

Conclusion

In this study a measurement circuit that can map fluidic resonances inside a printhead with low noise and high scanning speed has been developed. Functionality and reliability was proven.

The method of compensating electric behaviour of the actuator made the observation of the resonance peak possible and is the key addition to a current self sensing system to allow for viscosity measurements. The isolation amplifier has helped to greatly reduce the noise level of the measured signal and common mode rejection of the actuating sinusoidal wave and thus increase the accuracy and repeatability of the measurement.

By using the circuit and measuring method developed here, deviations in the ink viscosity in the printhead can be monitored directly without having to know the actual viscosity. In a further step, printheads can now be used directly as measurement devices for viscosity at very high frequencies above $100\,kHz$ that are dominant in piezo inkjet printheads. In-process monitoring of ink rheology at jetting relevant frequencies is possible for the first time to the best of our knowledge.

Following the results presented here, a circuit was developed which makes it possible to measure not only the amplitude of the resonance but also its phase. The phase can be used to determine the elasticity of a fluid. It is however difficult at this stage to point out the actual influence of a fluids elasticity on the phase measurement [9] and further research is being done.

References

[1] J. Frits Dijksman, *Design of Piezo Inkjet Print Heads*, Wiley-VCH Verlag GmbH, 2018.

[2] *Piezofibel: Theorie, Anleitung, Anwendung*, piezosystem jena, 1995.

[3] Suryanarayana Prasad a N, Quentin Gallas, Stephen Horowitz, Brian Homeijer, Bhavani Sankar, Louis Cattafesta, and Mark Sheplak, "Analytical electroacoustic model of a piezoelectric composite circular plate," *Aiaa Journal - AIAA J*, vol. 44, 10 2006.

[4] Kye-Si Kwon, "Methods for detecting air bubble in piezo inkjet dispensers," *Sensors and Actuators A: Physical*, vol. 153, no. 1, pp. 50–56, 2009.

[5] Byung-Hun Kim, Sang-Il Kim, Hyun-Ho Shin, Na-Rae Park, Hyun-Seok Lee, Chang-Soo Kang, Seung-Joo Shin, and Seong-Jin Kim, "A study of the jetting failure for self-detected piezoelectric inkjet printheads," *IEEE Sensors Journal*, vol. 11, no. 12, pp. 3451–3456, 2011.

[6] Kye-Si Kwon, Yun-Sik Choi, Dae-Yong Lee, Jeong-Seon Kim, and Dae-Sung Kim, "Low-cost and high speed monitoring system for a multi-nozzle piezo inkjet head," *Sensors and Actuators A: Physical*, vol. 180, pp. 154–165, 2012.

[7] A.J. Brown, "Spectral curve fitting for automatic hyperspectral data analysis," *IEEE Transactions on Geoscience and Remote Sensing*, vol. 44, no. 6, pp. 1601–1608, 2006.

[8] Piller Julian, "Sensing of fluid rheology in an inkjet printhead," 07 2021.

[9] Perritaz Gaël, "Printhead as high frequency rheometer with phase measurement," 07 2022.

Author Biography

Filliger Sebastian received a BSc in electronics from the University of applied science of Fribourg in 2016, after which he started working at iPrint while continuing his master studies in electronics at the University of Applied Science of Western Switzerland where he graduated in 2019. During his time at iPrint he worked in many fields around inkjet but later specialised in analogue and digital driving electronics for inkjet and started the research of piezo self-sensing for inkjet at iPrint.
Mail: sebastian.filliger@hefr.ch

Brügger Luca has obtained his Master of Science from the HES-SO in Electrical Engineering in 2023 and is now working as an R&D Engineer in Electronics at iPrint. During his studies he was already working on multiple student projects for iPrint and got well involved in inkjet technology and piezo self-sensing.
Mail: luca.bruegger@hefr.ch

Piller Julian and Perritaz Gaël both worked at iPrint and contributed extensively to the study during their respective bachelor theses.